American Journal of Engineering Research (AJER)
e-ISSN : 2320-0847 p-ISSN : 2320-0936
Volume-03, Issue-06, pp-323-339
www.ajer.org

Research Paper Open Access

Effect of Manganese Addition and the Initial Aspect Ratios on the Densification Mechanism/S and Barrelling In Sintered Hyper Eutectoid P/M Steel Preforms During Hot Upset Forging

[1] Hemlata Nayak, [2] C. M. Agrawal, [3] K. S. Pandey
[1]*PhD. Research Scholar, Department of Mechanical Engineering, Maulana Azad National Institute of Technology, Bhopal,Madhya Pradesh India.*
[2]*Formerly, Professor, Department of Mechanical Engineering, Maulana Azad National Institute of Technology, Bhopal, Madhya Pradesh India*
[3]Professor, *Department of Metallurgical and Materials Engineering National Institute of Technology, Tiruchirapalli-620015,Tamilnadu, India.*

ABSTRACT:- Present investigation pertains to evaluate the materials behaviour during hot upset forging of sintered hyper eutectoid P/M steels containing manganese and these steels are Fe-1.0%C-0.0%Mn, Fe-1.0%C-1.75%Mn,Fe-1.0%C,Fe-1.0%c-2.75%Mn and Fe-1.0%C-3.75%Mn respectively. These compositions from individual elemental powders were homogeneously blended separately in a potmill for a period of 36 hours. Preforms of initial aspect ratio of 0.43 and 0.83 with a diameter of 27.5mm were compacted to a density level of 85±1 per cent of theoretical by applying pressures in the range of 480±10 MPa and by taking pre-weighed powder blends. These compacts were coated with the indigenously developed ceramic coating to protect them against oxidation during sintering at 1150˚±10˚C in an electric muffle furnace for a period of ninety minutes. Once sintering schedule was completed, the sintered preforms of all compositions and both aspect ratios were hot upset forged to different height strains and then oil quenched. Quenched discs were thoroughly cleaned and dried. Initial and final dimensions of sintered and forged discs of all compositions were made including density measurements. Based on the initial parameters, various parameters were calculated such as true diameter and height strains, bulging ratios, relative densities, Poisson's ratios and diameter strains considering circular and parabolic bulging. Various plots were drawn among the calculated parameters and were critically analyzed. Critical analyses of these plots have yielded various empirical relationships fully describing the material behaviour during hot upset forging.

Keywords: - Aspect ratio, Blended, Compact, diameter, elemental, Forged, homogeneously, upset.

I. INTRODUCTION

Technically, the classification of alloy steels has been carried out in such a manner so as to consider the steel as low alloy if and only if, the total content of the alloying elements are lower than 5% and medium if the content ranges in between 5% to 10%, and, the steel is termed as high alloy steel if the steel contained the alloying elements beyond 10% [1]. It is true, that the plain carbon steels are quite satisfactory in various engineering applications subject to conditions that their strengths and other expectations are not, too, rigorous. Further it is reported that these steels can be employed in service where the temperature of applications is moderately low and the environments in which they are used is not, too, hostile. The major draw backs of these plain carbon steels have been successfully encountered by the addition of selective alloying elements. Therefore, the alloy steels can be redefined as the one whose basic characteristic properties are attributed to one or other alloying elements other than carbon. It has been also reported elsewhere [2] that several alloy steels do fulfil the strength requirements of a given application by inducing sufficient harden ability in the desired section size.

However, the exact options are limited by certain specific requirements such as low temperature toughness, creep resistance, corrosion or wear resistance including the freedom from temper embrittlement. It is reported [3] that manganese is one of the least expensive alloying elements and is virtually present in all steels as deoxidizer. Manganese is inherited with the characteristic features to reduce the tendency of hot-shortness resulting from the presence of sulphur, and, thus enabling the steel to be hot worked easily. Further manganese strengthens ferrite and is mild carbide former. Apart from the above, the manganese strengthens the steel in the as rolled condition and further imparts enhancement of strength and ductility to the steel in the heat treated condition. It is reported [4-15] that hot forging of P/M preforms is a highly developing process which can produce dense products from metal powders which are being employed in structural applications. P/M forging imparts improved densification coupled with a large amount of deformation in a single stroke of the punch of the press. It is also reported [16] that engineering parts can be produced to net shape with almost cent per cent dense via sintering the preforms followed by hot forging with high ductility. Apart from these, it has been conclusively established that the pores present in the component act as initiators of cracks under cyclic loading [17], and, therefore, there is a strong need to eliminate them by scientifically designed, fabricated and heat treated dies [18, 19].

Production of parts or components by powder preform forging (PPF) is an attractive process as it blends time, material and costs [20] saving advantages. The P/M preforms come under the category of porous materials experiencing plastic deformation when subjected to compressive loadings, thus, an increase in the achieved density. Technically, the magnitude of deforming blows and the dies associated with the conventional forgings are replaced by one blow and one die on a preform shaped from powder or powder blends by compaction followed by sintering. Thus, PPF is carried out in confined or closed dies which in turn ensures full densification and also eliminates the possibilities of flash formation [21]. In order to achieve mechanical properties equal to or superior to to conventionally produced parts, the P/M preforms must be designed to accommodate the metal flow and also the provision to eliminate any possibility of fracture. Another consideration must be made on the type of stresses and their stress levels required acquiring the final component or the part with full density while forming them for actual applications. Thus, these information would truly provide a real estimate of the stresses required, the press capacity to hot forge the desired component [22], and, hence, the process would provide the feasibility [23] to fabricate quite complex components in one forging operation, Therefore, engineering components can be manufactured to almost cent per cent density levels through powder or powder blend compaction and sintering followed by hot forging inducing fairly high ductility in the components.

Present investigation attempts to investigate the influence of manganese addition 0.0%, 1.75%, 2.75% and 3.75% respectively in Fe-1.0%C steel on the various aspects of densification, bulging, and Poisson's ratio under the conditions of normal, circular and parabolic modes of bulging considered during high temperature forgings of sintered P/M manganese steels.

II. EXPERIMENTAL DETAILS

II.1 Materials Required

Atomized iron powder of -180µm was procured from M/s. The Sundaram Fasteners Limited, Hyderabad, Andhra Pradesh, India. The manganese powder of -37µm was supplied by M/s. The Speciality Powders Pvt. Ltd., Mumbai, Maharashtra, India. However, the graphite powder of -5µm was provided by courtesy The M/s. Asbury Graphite Inc., New Jersey, U. S. A. The chemical analysis of the iron powder yielded a purity of 99.65% with 0.35% insoluble impurities whereas the chemical purity of manganese was found out to be 99.38% with an insoluble impurity content of 0.62%.The ash content of graphite powder was found to be 1.79%, i.e., remaining 98.21% was the effective carbon content. The basic characteristics of the respective powder blends are given in Table 1. However, the sieve size analysis of the base powder, i.e., iron is provided Table 2. High Carbon and High Chromium (HCHC) steel was required to fabricate the

Table 1 Characterization of Iron Powder and Powder Blends

Systems	Apparent Density, g/cc	Flow rate, S/100g.	Compressibility, g/cc at a pressure of 480±10MPa.
Fe-1.0%C	2.89	63	6.37
Fe-1.0%C-1.75%Mn	2.84	67	6.32
Fe-1.0%C-2.75%Mn	2.80	69	6.24
Fe-1.0%C-3.75%Mn	2.77	73	6.13

compaction die set assembly. The compaction assembly included was the mother die, the punch and the bottom insert. These die parts have been machined from suitable blanks, heat treated in the range of 950º±10ºC for one hour to four hours depending upon the part keeping in mind that every 25mm diameter part was heated and soaked for one hour at the above temperature and quenched in oil. The hardness values were in the range of 59-61Rc. These parts were tempered to hardness values of 54-56Rc. Powder compaction was carried out using 1.0MN capacity Universal Testing Machine. Apart from these, an electric muffle furnace was required to be used during sintering the compacts, which was kept near the Friction Screw Press of 1.0 MN capacity. This press was subsequently used for hot upset forging the above steels. The die material selected for the hot dies was Molybdenum die steel which are having the rectangular dimensions of 240 mm X150 mm X 100mm.

Table 2 Sieve Size Analysis of Iron Powder

Powder Sieve Size, µm	-180 + 150	-150 +125	-125 +106	-106 +90	-90 +75	-75 +63	-63 +53	-53 +37	-37
Wt% powder retained	1.52	1.83	23.12	1.11	21.86	2.21	18.60	13.62	**16.11**
Cum. Wt% powder retained	**1.52**	**3.35**	**26.47**	**27.58**	**49.44**	**51.65**	**70.25**	**83.87**	**99.98**

II.2 Blending of Mixes of Elemental Powders

Powder mixes corresponding to yield the steel compositions, namely, Fe-1%C-0.0%Mn, Fe-1.0%C-0.0%Mn, Fe-1.0%C-1.75%Mn, Fe-1.0%C, Fe-1.0%c-2.75%Mn and Fe-1.0%C-3.75%Mn respectively were blended in a separate pots on a pot mill for a period of 36 hours. Initially pre-weighed elemental powders corresponding to yield the above compositions were kept in separate pots with powder mix to porcelain balls of 15-20mm diameters in the weight ratio of 1.1:1 and the pot lids were securely tightened and fixed on the pot mill and mill was switched on. At an interval of every one hour the pot mill was switched off and nearly 110 g of powder mix from each pot was taken out and measurements such as flow rates and apparent densities were measured. Once, this operation was completed, the powder mixes were returned back to the respective pots and their respective lids were tightened properly and the pots were re-fixed on the pot mill and the mill was switched on again. This schedule was continued till the lost three observations of flow rates and apparent densities were consistent. It was found out that the blending time of 36 hours was most suitable to yield homogeneous blends for each mix. Thus, the blending time was fixed as 36 hours for each powder mix. Now, the powder blends were ready for compact preparations.

II.3 Compaction of Powder lends

Compaction of Powder Blends Powder blends corresponding to Fe-1.0%C-0.0%Mn, Fe-1.0%C-1.75%Mn, Fe-1.0%C, Fe-1.0%C-2.75%Mn and Fe-1.0%C, Fe-1.0%C-3.75%Mn compositions were accurately weighed for

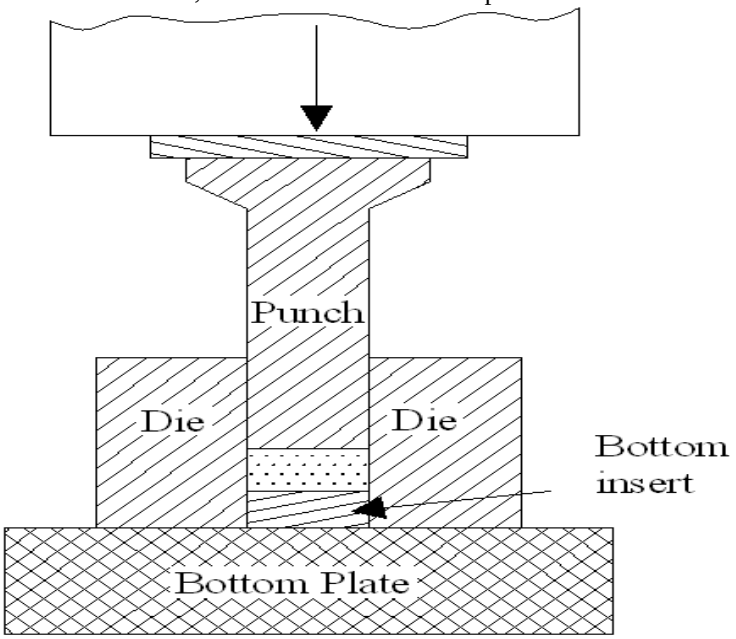

Figure 1 Schematic Diagram of Complete Compaction Assembly.

Compact preparations of initial aspect ratios of 0.43, and 0.83 respectively. Compacts of above initial aspect ratios were prepared by using Universal Testing Machine of 1.0 MN capacity and suitable die set assembly. The preform densities were maintained in the range of 85±1 per cent of theoretical by applying the pressure in the range of480±10 MPa The diameter of the compaction die was $24.84^{\pm 0.01}$ mm. Graphite powder with acetone as a paste was employed as lubricant during compaction. Powder compaction assembly is shown in figure 1. A minimum of 12 compacts of each aspect ratios and for all four compositions were prepared.

II.4 Application of Indigenously Developed Ceramic Coating

Indigenously developed ceramic coating [24] was applied on the entire surfaces of all the compacts to protect them against oxidation during sintering in the temperature range of 1150 ± 10^0C for a period of ninety minutes and subsequently transferring them to the bottom die of the friction screw press for hot upset forging. The ceramic coating was applied on the entire compact surfaces of all the compacts and the same was allowed to dry for a period of i6 hours in an ambient conditions. All coated compacts were recoated perpendicular to the direction of the previous coating and this, coating, too, was allowed to dry for a further period of 16 hours under the aforementioned ambient conditions. Now the coated compacts were ready for further processing.

II.5 Sintering of Ceramic Coated Compacts

Once the drying operation was completed, twenty-four (24) compacts of one composition were kept in a rectangular ceramic tray and the tray was charged inside the electric muffle furnace. The furnace was switched on and the temperature was raised to 750º±10ºC and retained at this temperature for a period of 50 minutes to allow the volatile ingredients to come out. Immediately after this the furnace temperature was raised to 1150 ± 10ºC and this temperature was retained for a period of ninety minutes. This completes the sintering schedule. Now, the sintered compacts were ready to undergo the next step of operation. Same step was followed for each composition so as to maintain the identity of each composition.

II.6 Hot Upset Forging of Sintered Compacts

All sintered compacts except two of each aspect ratio, namely, 0.43, and 0.83 respectively of each composition were hot upset forged to different height strains on a 1.0MN capacity friction screw press using flat molybdenum die steel plates. Immediately after hot upset forging, the sintered preforms, forged discs were quenched in linseed oil bath so as to retain the sintered and forged structures whichever is the case.

II.7 Removal of Residual Ceramic Coating From All the Oil Quenched

Residual ceramic coatings from the sintered oil quenched and forged oil quenched were removed by mild machining/grinding or by mild filing or by using abrasive papers ensuring that no metal is abraded out. This procedure was employed to all the forged preforms of disc shaped of all compositions and all aspect ratios. This adoption of removal of ceramic coating would bring high order of uniformity as well as the accuracy in density measurements along with their actual forged dimensions.

II.8 Dimensional Measurements of Cleaned sintered and Forged Discs and the Different Required Parameters to be calculated.

The measurements of the initial parameters like forged height, contact diameters (D_{ct} and D_{cb}), bulged diameter (Db), density and the other parameters for the calculation of such as True Height Strain $\{\varepsilon_h=(\ln H_o/H_f)\}$, True Diameter Strains, namely, conventional $\varepsilon_d = \{\ln (D_{cf} /D_o)\}$, diameter strain for circular arc of barrelling, $\varepsilon_{dcb}= \{(\ln[(2D_b^2+D_{cf}^2)/(3D_0^2)])/2\}$, diameter strain for parabolic arc of barrelling; $\varepsilon_{dpb}= \{(\ln[(8D_b^2+4D_bD_{cf}+3D_c^2)/(15D_0^2)])/2\}$ respectively, Bulging Ratio (D_b/D_o), and the Poisson's Ratios, conventional $[\{\ln (D_{cf} /D_o)\}/2\{\ln (H_0/H_f)\}]$, Poisson's Ratio differently defined by Narayanasamy and Pandey along with others were calculated [25-28] for circular arc of barrelling $[\{\ln[(2D_b^2+D_{cf}^2)/(3D_0^2)]\}/\{2 \ln(H_0/H_f)\}]$ and Poisson's Ratio for parabolic arc of barrelling $[\{\ln[(8D_b^2+4D_bD_{cf}+3D_{cf}^2)/(15D_0^2)]\}/\{2 \ln(H_0/H_f)\}]$ and also the evaluation of fractional theoretical density to investigate the various aspects of densification behaviour has been carried out.

II.9 Density Measurements of sintered and forged Discs

Density measurements of all the forged and cleaned compacts were found out by employing Archimedean principle [15] whereas, the density of sintered compacts were found out by calculating the volume geometrically and the mass in air using Adair-180 electronic balance with a sensitivity of 10^{-4}. A very fine water repellent oil film [17] was employed on all the forged compacts so as to avoid the penetration of water into the pores, thus, not affecting the calculations of the true volumes of the forged compacts. Typical formula used is given as under:

ρ_f, g/cc = $\{M_{air}/(M_{air} - M_{water})\} \times \rho_{water}$ .....(1)

Where, M_{air} = Mass of the forged disc in air in g, M_{water} = Mass of the forged disc in water in g, and, ρ_{water} is the density of water. Density correction was introduced depending upon the room temperature by using standard chart for density variation of water with respect to temperature.

II.10 **Various Plots Drawn for Analysis of Experimental Data and Calculated Parameters**

In order to arrive at a fruitful conclusion of the present investigation various plots were drawn, and, the same were critically analysed which yielded various empirical relationships correlating relevant parameters, and, thus, expressing them through various mathematical equations. The plots that were drawn are among the various parameters are (1) Relative density V/s. True height strain; Relative density V/s. True diameter strain; Relative density V/s. True diameter strain with circular barrelling and relative density V/s.True diameter strain for parabolic barrelling, Poisson's Ratio against fractional theoretical densities, fractional theoretical densities V/s.bulging ratio (D_b/D_0), Log (%fractional theoretical density) V/s. Log (D_b/D_0) and the bulge ratio against per cent theoretical densities were plotted in order to evaluate the complete densification mechanism/s.

III. RESULTS AND DISCUSSION

III.1 Deformation and Densification

Fig. 4 shows the plots drawn between relative density (ρ_f/ρ_{th}) and the true height strains(ln (H_0 /H_f)) exhibiting the influence of initial preform geometry and the compositions of the steels. Irrespective of the composition of the steel, the lower aspect ratio preforms densified at a much faster pace compared to the larger aspect ratio preforms. This is attributed to the fact that during hot upset forging the load transfer across the axial direction is quite rapid and uniform in lower aspect ratio preforms due to lower level of resistance

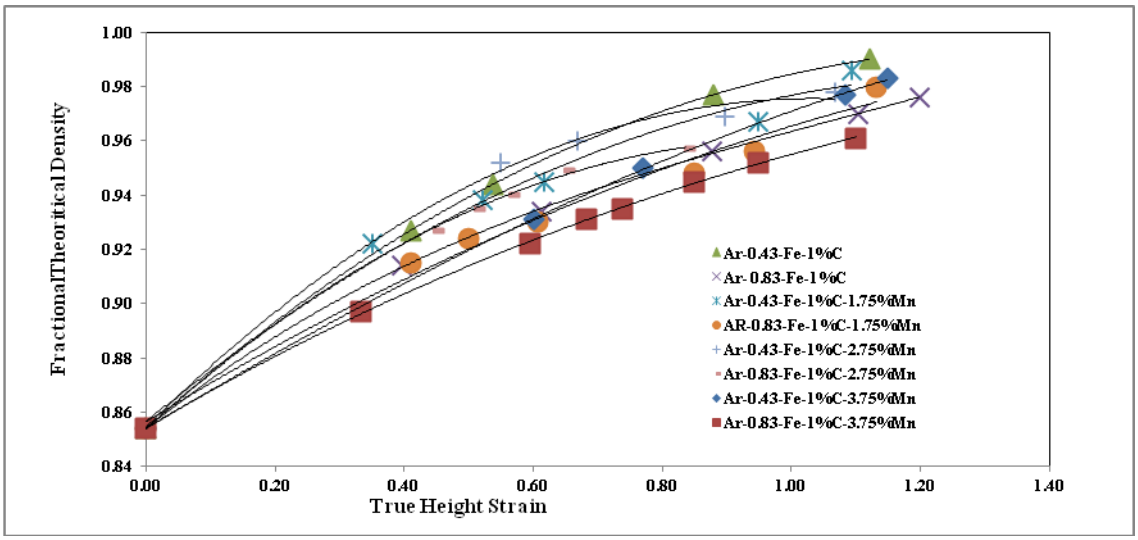

Figure 4 Effect of Initial Aspect Ratio (H_0/D_0) On the Relationship between Fractional Theoretical Densities and True Height Strains.

Offered by them against deformation as compared to the larger aspect ratio preforms which offered higher level of resistance. Further, this can be associated to the fact that lower aspect ratio preforms contained lower level of pore bed as compared to larger aspect ratio preforms which contained higher level of pore bed and hence offered enhanced resistance to deformation and densification. All curves in this figure are found to be quite similar to each other in nature, and, therefore, they all must be represented by a similar mathematical expression. The curve fitting technique employed for these curves have yielded a third order polynomial of the form as given in equation (1) to which they conformed to is given beneath:

$$(\rho_f/\rho_{th}) = a_0 + a_1\epsilon_h + a_2\epsilon_h^2 + a_3\epsilon_h^3 \text{.....} \quad (2)$$

Where, 'a_0', 'a_1', 'a_2', and 'a_3' were found to be empirically determined constants but were found to depend upon initial preform geometry and the steel compositions. All these constants are tabulated in Table 3. Examining Table 3 carefully, it is found that the constant 'a_o' is in very much in close proximity to initial relative density (ρ_0/ρ_{th}) of the preforms. Hence, this constant did not contribute to the densification at all. However, the constant

Table 3 Coefficients of third order polynomial of the form: $(\rho_f/\rho_{th}) = a_0 + a_1\epsilon_h + a_2\epsilon_h^2 + a_3\epsilon_h^3$; $\epsilon_h = \ln(H_0/H_f)$

Composition	Coefficients of the third order polynomial					Regression Coefficient
	H_0/D_0	a_o	a_1	a_2	a_3	R^2
Fe - 1.0%C	0.43	0.854	0.213	-0.089	0.006	1.000
	0.83	0.854	0.190	-0.116	0.035	0.999
Fe - 1.0%C - 1.75Mn	0.43	0.846	0.336	-0.409	0.200	1.000
	0.83	0.844	0.274	-0.309	0.152	0.999
Fe - 1.0%C - 2.75%Mn	0.43	0.846	0.357	-0.383	0.154	1.000
	0.83	0.845	0.222	-0.065	-0.047	0.999
Fe - 1.0%C - 3.75%Mn	0.43	0.854	0.141	-0.016	-0.007	0.999
	0.83	0.854	0.141	-0.046	0.005	0.999

'a_1' is linearly multiplied to the true height strain and has always remained positive, and, therefore, this contributed to densification linearly. But, the constant 'a_2' is negative and is multiplied to the square of the true height strain which in general has been less than unity and, therefore, its square will be much less than unity and the product of 'a_2' and the square of the true height strain would become negligibly small. Obviously, this constant would literally moderate the densification curves in the final stages of deformation, i.e., the curves would tend to plateau. Similarly the constant 'a_3' is either positive or negative, but of a low magnitude and, hence, its effect in densification is negligibly small. Thus, the major contribution to densification is associated with the constant 'a_1'. However, the values of constants 'a_2' and 'a_3' only assisted to densification mechanism in such a manner so as to plateau the densification curves in the final stages of densification. Apart from this, the values of regression coefficient 'R^2', is found to be either unity or very much close to unity, and, hence, the densification curves are the best fit curves. Therefore, the proposed empirical relationship stands justified.

III.2 Deformation, Densification and Diameter strains

Figs. 5, 6 and 7 represent the plots between the relative density (ρ_f/ρ_{th}) and the true diameter strains for conventional (fig.5),for circular barrelling, (ε_{dcb}), (fig.6) and for parabolic barrelling, (ε_{dpb}), (fig.7) respectively. Curves shown in the figures 5 and 6 are found to be similar in characteristic nature and are further found to conform to a second order polynomial of the form:

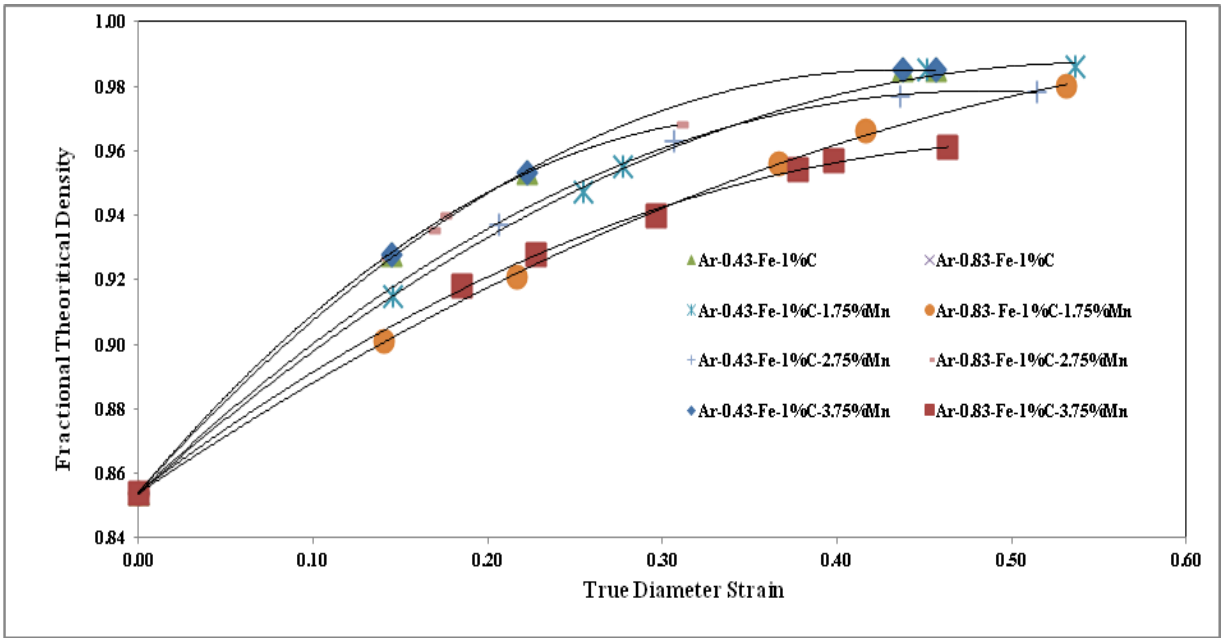

Figure 5 Effect of Initial Aspect Ratio (H_0/D_0) on the Relationship between Fractional Theoretical Densities and the True Diameter Strain.

Table 4 Coefficient of the polynomial of the form: $\rho_f/\rho_{th} = b_0\varepsilon_d + b_1\varepsilon_d + b_2\varepsilon_d^2$

Composition	H/D	b_0	b_1	$-b_2$	R^2
Fe-1%C	0.43	0.854	0.6	0.689	0.999
	0.83	0.854	0.411	0.389	0.999
Fe-1%C-1.75%Mn	0.43	0.846	0.531	0.504	0.999
	0.83	0.846	0.413	0.308	0.999
Fe-1%C-2.75%Mn	0.43	0.846	0.563	0.598	0.999
	0.83	0.845	0.727	1.067	0.999
Fe-1%C-3.75%Mn	0.43	0.854	0.600	0.689	0.999
	0.83	0.854	0.411	0.389	0.999

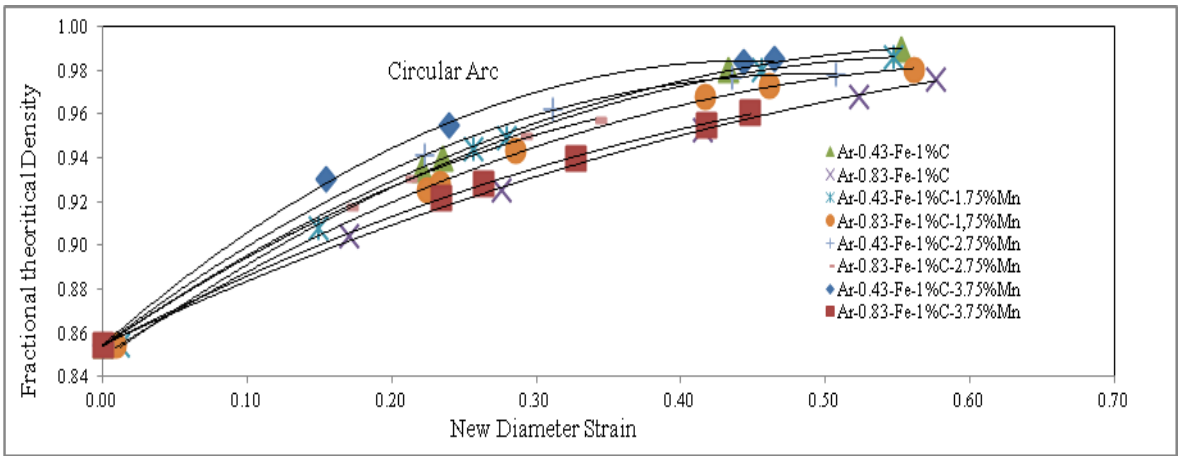

Figure 6 Effect of Initial Aspect Ratio (H_0/D_0) on the Relationship between Fractional Theoretical Densities and New Diameter Strains for Circular Arc.

Table 5 Coefficient of the polynomial of the form: $\rho_f/\rho_{th} = c_0\varepsilon_{dc} + c_1\varepsilon_{dc} - c_2\varepsilon_{dc}^2$

Composition	H/D	c_0	c_1	$-c_2$	R^2
Fe-1%C	0.43	0.854	0.451	0.371	1
	0.83	0.854	0.307	0.170	0.99
Fe-1%C-1.75%Mn	0.43	0.839	0.523	0.471	0.99
	0.83	0.839	0.472	0.394	0.99
Fe-1%C-2.75%Mn	0.43	0.846	0.553	0.578	1
	0.83	0.844	0.523	0.566	0.99
Fe-1.0%C-3.75%Mn	0.43	0.854	0.578	0.643	0.99
	0.83	0.854	0.341	0.235	0.99

$$(\rho_f/\rho_{th}) = b_0 + b_1\epsilon_d + b_2\epsilon_d^2 \text{ -------} \quad \text{-------- -------- ----- (3), and,}$$

$$(\rho_f/\rho_{th}) = c_0 + c_1\epsilon_{dcb} + c_2\epsilon_{dcb}^2 \text{ ... ...} \quad \text{..... (4)}$$

Where, $\epsilon_d = \ln(D_c/D_0)$ and $\varepsilon_{dcb} = \{(\ln[(2D_b^2+D_{cf}^2)/(3D_0^2)])/2\}$, respectively. All these constants b_0, b_1, b_2, c_0, c_1, and c_2 are tabulated in Tables 4 and 5 respectively. The constants b_0 and c_0 do not contribute to densification as they are in close proximity of the initial preform relative densities (ρ_0/ρ_{th}), whereas the constants b_1 and c_1 are linearly multiplied to the respective true diameter strains and hence assisted to densification linearly as all of them were positive irrespective of compositions and the initial preform geometries. However, the constants b_2 and c_2 are all negative but of low magnitude and are multiplied to square of true respective diameter strains which itself is much less than unity, and, hence, these constants only assisted in the flattening of the curves in the final stages of deformation and densification. This is true, irrespective of the composition and the initial preform geometries. Similarly, fig.7 is drawn between the relative density (ρ_f/ρ_{th}) and the new diameter strain considering the parabolic form of barrelling. Since, all the curves in this figure are found to be similar in characteristic nature, and, therefore, they must be represented by a similar mathematical expression.

Hence, an attempt has been made to assess the curve fittings appropriately. The employed curve fitting technique has yielded a third order polynomial of the form:

$$(\rho_f/\rho_{th}) = d_o + d_1\epsilon_{dp} + d_2\epsilon_{dpb}^2 + d_3\epsilon_{dpb}^3 \text{------ ------- ----- (5)}$$

Where, d_0, d_1, d_2 and d_3 are empirically determined constants and are found to depend upon initial preform geometries and the compositions of the steels investigated in the present study. These constants are tabulated in Table 6. The constant 'd_0' in each case is found to be in close proximity to the initial preform densities and, therefore, did not contribute to densification in any form. However, the constant values of 'd_1' and 'd_3' are positive, and, therefore, they assist in enhancing the forged densities as the deformations are advanced. But, the constant values of 'a_2' are found to be all negative, and, therefore, they tend to flatten the curves in their final stages of journey. Since, the values of the regression coefficient 'R^2' are found to be unity in each case, and, therefore, it is conclusively established that the consideration of parabolic barrelling during hot upset forging is highly pronounced.

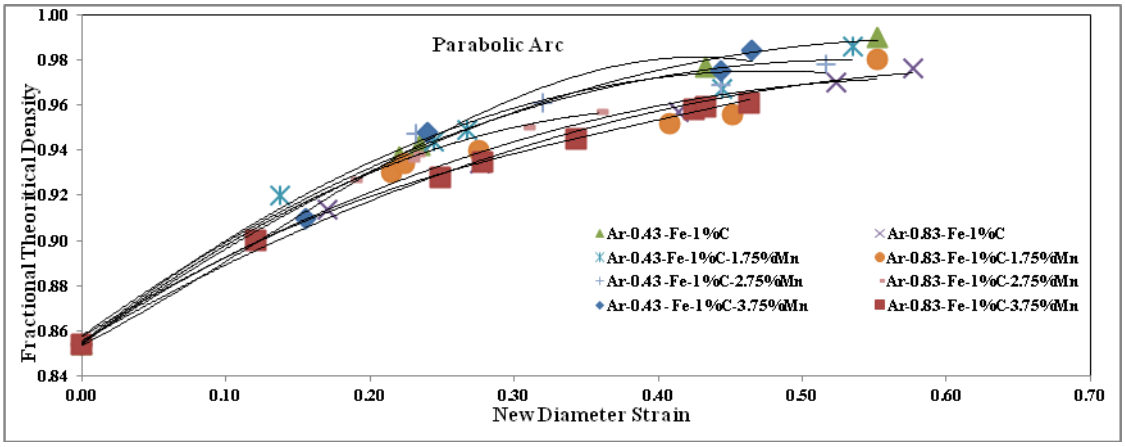

Figure 7 Effect of Initial Aspect Ratio (H_0/D_0) on the Relationship between Fractional Theoretical Density and New Diameter Strain for Parabolic Arc.

Table 6 Coefficient of the polynomial of $(\rho_f/\rho_{th}) = d_0\varepsilon_{dp} + d_1\varepsilon_{dp} - d_2\varepsilon_{dp}^2 + d_3\varepsilon_{dp}^3$

Composition	H/D	d_0	d_1	$-d_2$	d_3	R^2
Fe-1%C	0.43	0.85	0.51	0.70	0.39	1.00
	0.83	0.85	0.44	0.67	0.46	1.00
Fe-1%C-1.75%Mn	0.43	0.85	0.77	1.95	1.87	1.00
	0.83	0.84	0.73	1.90	1.85	1.00
Fe-1%C-2.75%Mn	0.43	0.85	0.77	1.75	1.48	1.00
	0.83	0.85	0.66	1.44	1.29	1.00
Fe-1%C-3.75%Mn	0.43	0.85	0.83	2.53	2.88	1.00
	0.83	0.85	0.51	1.28	1.43	1.00

III.3 Deformation, Densification and the Poisson's Ratio

Figs. 8, 9 and 10 are drawn between the Poisson's ratio, υ_{pg}, υ_{pc} and υ_{pp} respectively and the relative density (ρ_f/ρ_{th}). Observing these figures carefully, it is found that all the curves in each of the above figures 8, 9 and 10 are similar in their characteristic natures and, therefore, they all must be expressed by a similar mathematical expression. Curve fittings have yielded a second order polynomial between the Poisson's ratios (υ_{pg}, υ_{pc} and υ_{pp}) and the relative density (ρ_f/ρ_{th}). Thus, these expressions have the following forms:

For General Deformation:

$$\upsilon_{pg} = f_0 + f_1(\rho_f/\rho_{th}) + f_2(\rho_f/\rho_{th})^2, \quad \text{... ... ... (6)}$$

For Circular Barrelling:

$$\upsilon_{pc} = g_0 + g_1(\rho_f/\rho_{th}) + g_2(\rho_f/\rho_{th})^2, \quad \text{... ... ... (7)}$$

For Parabolic Barrelling:

$$\upsilon_{pp} = l_0 + l_1(\rho_f/\rho_{th}) + l_2(\rho_f/\rho_{th})^2 \quad \text{... ... ... (8)}$$

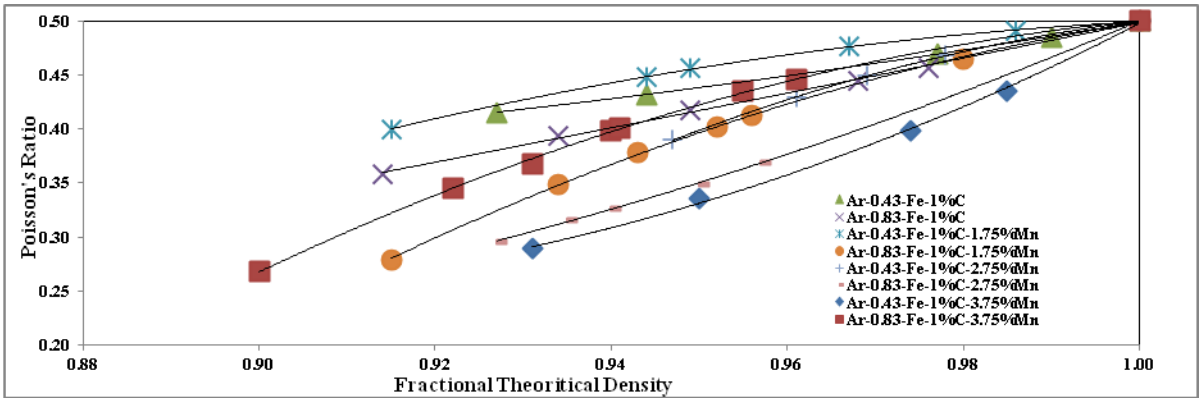

Figure 8 Effect of Initial Aspect Ratio (H_0/D_0) on the Relationship between Conventional Poisson's Ratio and Fractional Theoretical Density.

Table 7 Coefficient of the polynomial of the form: $\gamma = f_0 (\rho_f/\rho_{th}) + f_1(\rho_f/\rho_{th}) + f_2(\rho_f/\rho_{th})^2$ for Considering no Barrellings.

Composition	H/D	f_0	f_1	f_2	R^2
Fe-1%C	0.43	2.34	-5.06	3.22	1.00
	0.83	-0.76	0.86	0.40	1.00
Fe-1%C-1.75%Mn	0.43	-8.84	18.28	-8.93	1.00
	0.83	-15.93	31.57	-15.14	1.00
Fe-1%C-2.75%Mn	0.43	-20.57	41.13	-20.05	1.00
	0.83	6.01	-14.46	8.95	1.00
Fe-1%C-3.75%Mn	0.43	33.67	-72.79	39.62	1.00
	0.83	-15.62	31.45	-15.32	1.00

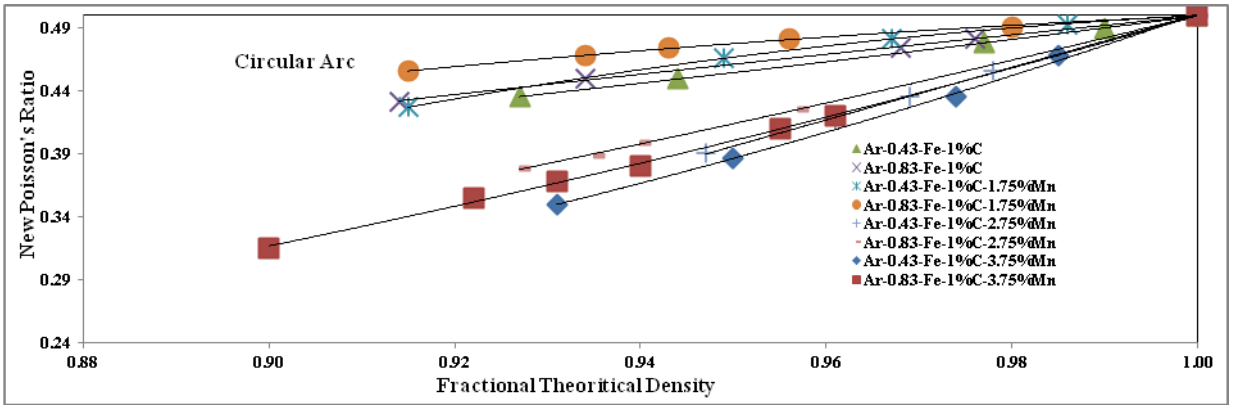

Figure 9 Effect of Initial Aspect Ratio (H_0/D_0) on the Relationship between New Poisson's and Fractional Theoretical Density for Circular Arc.

Table 8 Coefficient of the polynomial of the form: $\gamma_p' = g_0 (\rho_f/\rho_{th}) + g_1(\rho_f/\rho_{th}) + g_2(\rho_f/\rho_{th})^2$ for Circular Arc of Barrelling.

Composition	H/D	g_0	g_1	g_2	R^2
Fe-1%C	0.43	0.53	-1.02	0.98	1.00
	0.83	0.68	1.61	-0.43	1.00
Fe-1%C-1.75%Mn	0.43	-5.45	11.52	-5.57	1.00
	0.83	-1.91	4.48	-2.07	1.00
Fe-1%C-2.75%Mn	0.43	-1.53	1.97	0.06	1.00
	0.83	-2.28	-2.28	2.05	1.00
Fe-1%C- 3.65%Mn	0.43	13.34	-30.36	17.52	1.00
	0.83	1.46	-4.06	3.10	1.00

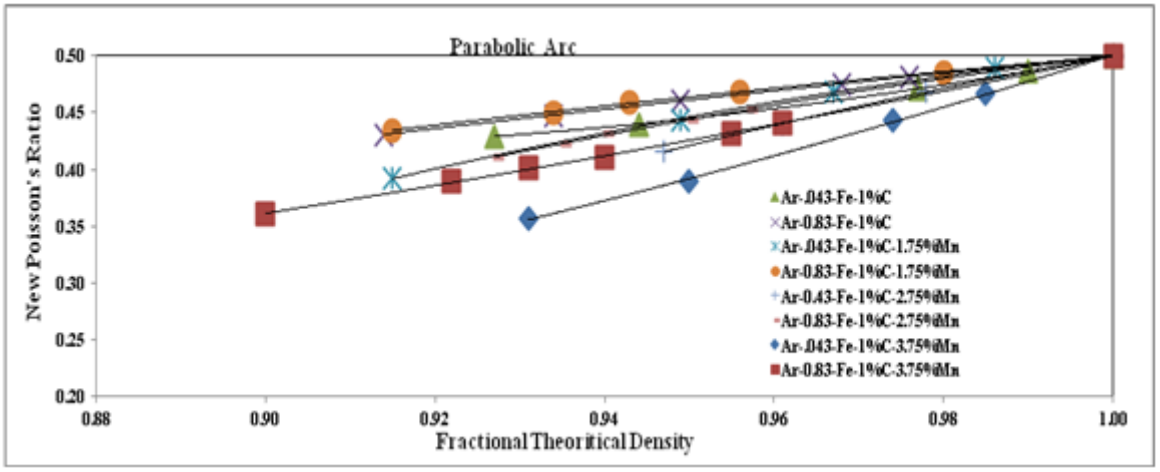

Figure 10 Effect of Initial Aspect Ratio (Ho/Do) and Fractional Theoretical Density for Parabolic Arc.

Table 9 Coefficient of the polynomial of the form: $\gamma_p'' = i_0 (\rho_f/\rho_{th}) + i_1(\rho_f/\rho_{th}) + i_2(\rho_f/\rho_{th})^2$ for Parabolic Arc.

Composition	H/D	i_0	i_1	i_2	R^2
Fe-1%C	0.43	4.87	-10.13	5.76	1.00
	0.83	-1.04	2.34	0.80	1.00
Fe-1%C-1.75%Mn	0.43	-5.84	11.88	-5.54	1.00
	0.83	-1.51	3.36	-1.35	1.00
Fe-1%C-2.75%Mn	0.43	-5.91	11.50	-5.08	1.00
	0.83	-4.73	9.56	-4.33	1.00
Fe-1%C-3.75%Mn	0.43	18.93	-41.64	23.22	1.00
	0.83	0.91	-2.41	2.00	1.00

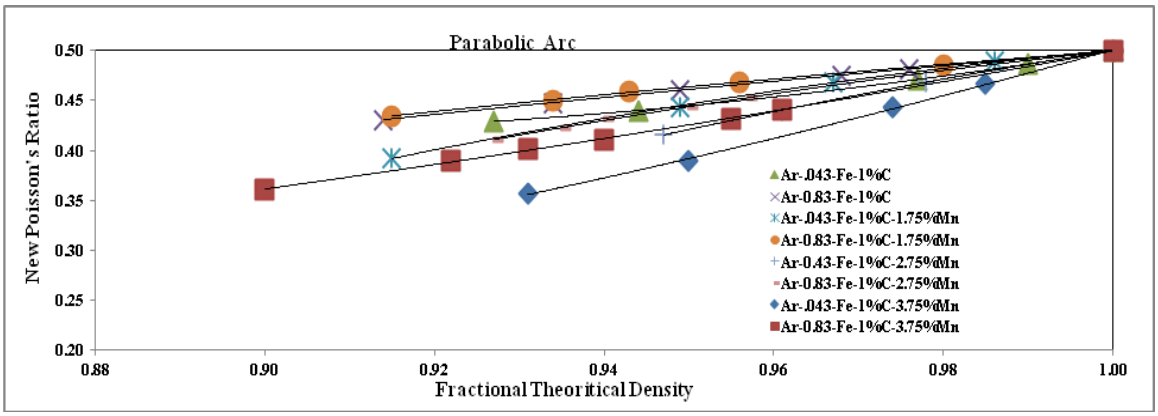

Where, f_0, f_1, f_2, g_0, g_1, g_2, l_0, l_1 and l_2 are empirically determined constants. All these constants are tabulated in Tables 7, 8 and 9 respectively for each aspect ratio and for each composition. These constants have not followed any set pattern instead either one is negative and two are positive or one is positive and the other two are (-) ve.

Since the values of regression coefficients (R^2) in each case is found to be unity, and, therefore, it can be taken for granted that the above proposed empirical relationships for Poisson's ratio against the relative density are the most ideal ones. Further it is found that in the near vicinity of cent per cent densification, the Poisson's ratio value attained had been 0.50 which is the case in the event of an ideal deformation where no barrelling is encountered.

III.4 Deformation, Densifications and Strains

Figs. 11, 12 and 13 are drawn between the true diameter strains (ϵ_{dg}, ϵ_{dc} and ϵ_{dp}) and the true height strains [ln (H_0/H_f)] where, ϵ_{dg} is the general true diameter strain without considering any barrelling; ϵ_{dc} is the true

diameter strain considering circular barrelling whereas, ϵ_{dp} is the true diameter strain considering parabolic barrelling. All data points in each figure for all aspect ratios and for all compositions lie below the theoretical line representing ideal deformation. All the curves corresponding to each aspect ratio and for each composition in each of the figures 11, 12 and 13 are similar in characteristic nature and the curve fitting has yielded second order polynomials of the form as beneath:

III.4.1 When No Barrelling considered

$$\epsilon_{dg} = j_0 + j_1 \epsilon_h + j_2 \epsilon_h^2 \quad \text{..... ....} \quad (9)$$

III .4.2 When Circular Barrelling considered

$$\epsilon_{dc} = k_0 + k_1 \epsilon_h + k_2 \epsilon_h^2 \quad \text{.... ....} \quad (10)$$

III.4.3 When Parabolic Barrelling considered

$$\epsilon_{dp} = m_0 + m_1 \epsilon_h + m_2 \epsilon_h^2 \quad \text{..... ... ...} \quad (11)$$

where , j_0, j_1, j_2, k_0, k_1, k_2, m_0, m_1 and m_2 are empirically determined constants and are found to depend upon the initial preform geometry and the compositions of the steels investigated. All these constants are tabulated in Tables 10, 11 and 12 respectively. Since the values of j_0, k_0 and m_0 are in close proximity to zero and hence do not contribute to true diameter strain on deformation because at no deformation there is no diameter strain or height strain. Hence, these constants are taken to be zero. j_1, k_1 and m_1 are all positive and are linearly multiplied

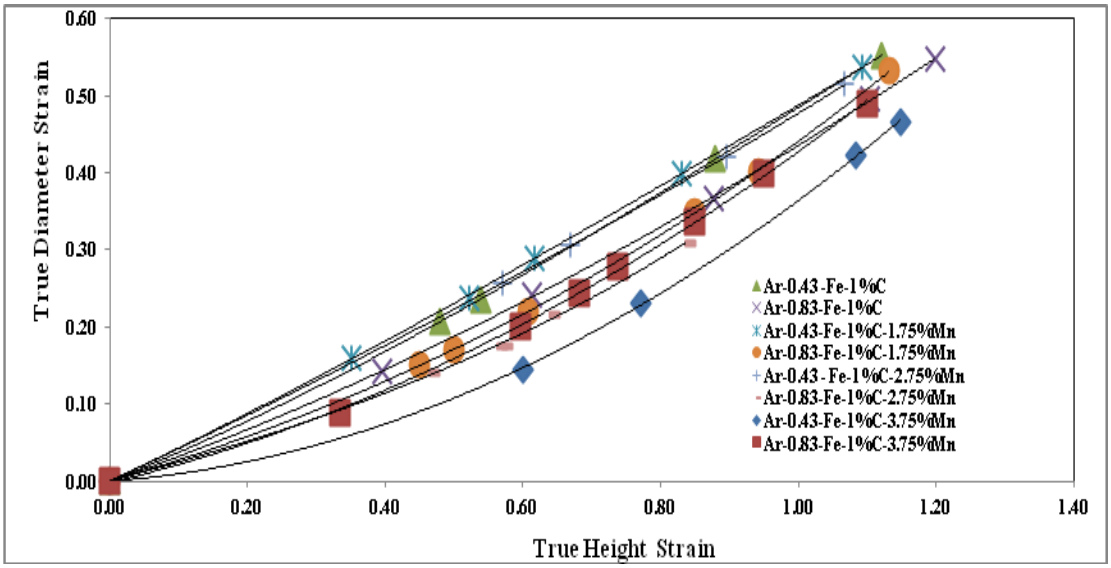

Figure 11 Effect of Initial Aspect Ratio (H_0/D_0) on the Relationship between True Diameter Strain and True Height Strain

Table 10 Coefficient of the polynomial of the form: $\varepsilon_{dnew} = j_0 (\varepsilon_h) + j_1 (\varepsilon_h) + j_2 (\varepsilon_h)^2$

Composition	H/D	j_0	j_1	j_2	R^2
Fe-1%C	0.43	0.001	0.391	0.092	1.0
	0.83	0.001	0.319	0.116	1.0
Fe-1%C-1.75%Mn	0.43	0.000	0.438	0.049	1.0
	0.83	0.000	0.239	0.202	0.99
Fe-1%C-2.75%Mn	0.43	-0.001	0.414	0.064	1.0
	0.83	0.000	0.198	0.205	0.99
Fe-1%C-3.75%Mn	0.43	-0.002	0.215	0.215	1.00
	0.83	0.000	0.068	0.296	0.99

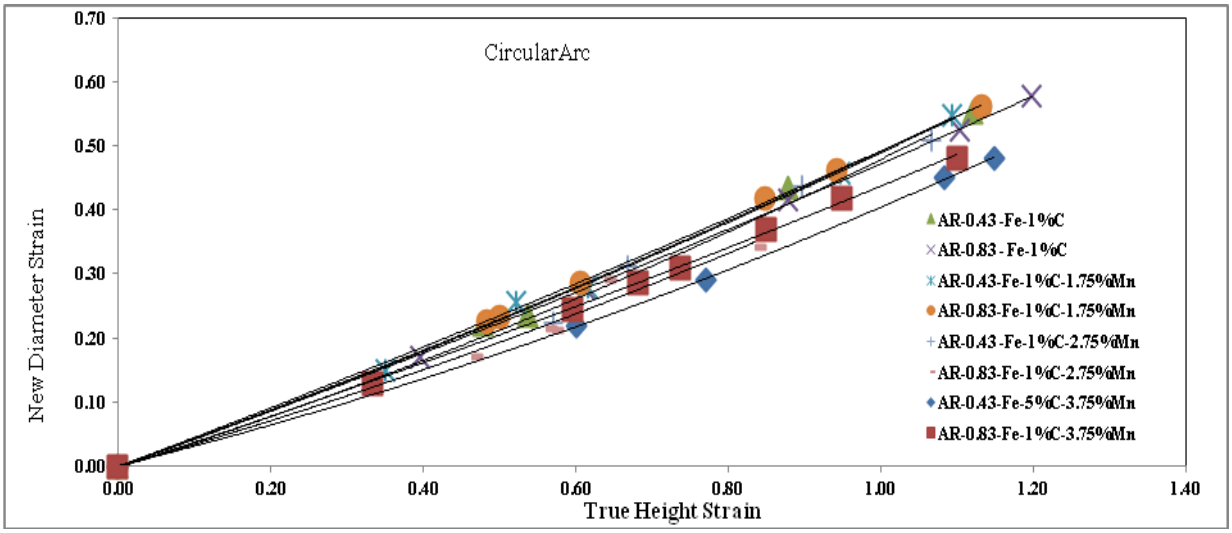

Figure 12 Effect of Initial Aspect Ratio (H_0/D_0) on the Relationship between New Diameter Strain and True Height Strain for Circular Arc

Table 11 Coefficients of the polynomial of the form: $\varepsilon_{dnewc} = k_0 (\varepsilon_h) + k_1 (\varepsilon_h) + k_2(\varepsilon_h)^2$

Composition	H/D	k_0	k_1	k_2	R^2
Fe-1%C	0.43	-0.001	0.42	0.07	1.00
	0.83	-0.001	0.42	0.05	1.00
Fe-1%C-1.75%Mn	0.43	-0.0001	0.43	0.06	1.00
	0.83	-0.0001	0.45	0.04	1.00
Fe-1%C-2.75%Mn	0.43	-0.002	0.38	0.11	0.99
	0.83	-0.001	0.34	0.09	0.98
Fe-1%C-3.75%Mn	0.43	0.001	0.11	0.26	1.00
	0.83	-0.002	0.39	0.05	1.00

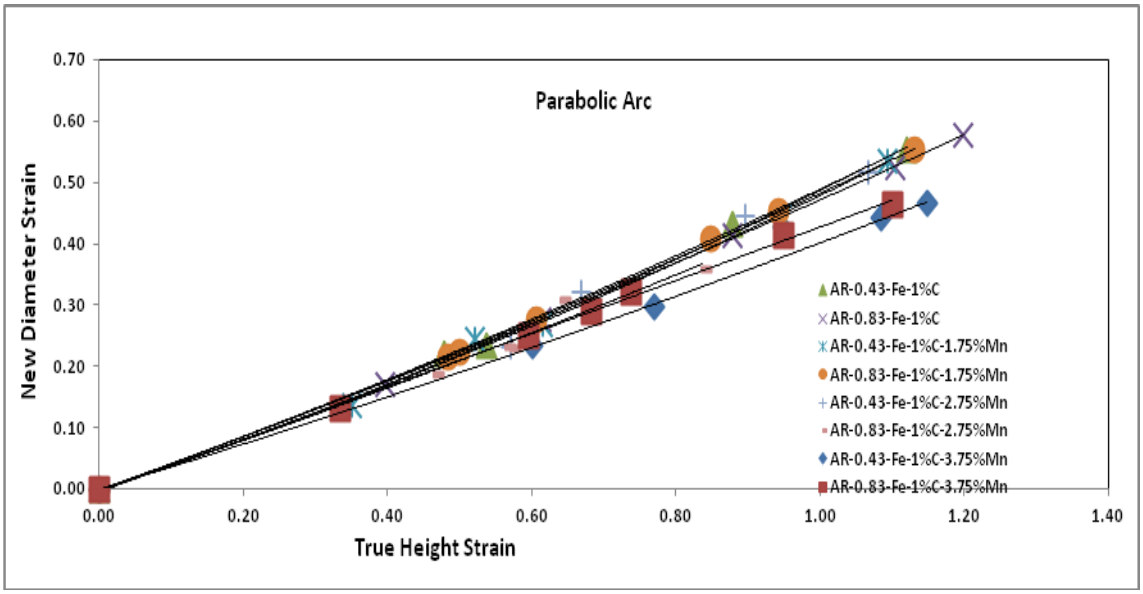

Figure 13 Effect of Initial Aspect Ratio (H_0/D_0) on the Relationship between New Diameter Strain and True Height Strain for Parabolic Arc.

Table 12 Coefficient of the polynomial of the form: $\varepsilon_{dnewp} = -l_0 (\varepsilon_h) + l_1 (\varepsilon_h) + l_2 (\varepsilon_h)^2$

Composition	H/D	$-l_0$	l_1	l_2	R^2
Fe-1%C	0.43	0.001	0.424	0.066	0.999
	0.83	0.001	0.423	0.048	0.999
Fe-1%C-1.75%Mn	0.43	0.001	0.391	0.087	0.997
	0.83	0.001	0.422	0.060	0.999
Fe-1%C-2.75%Mn	0.43	0.002	0.397	0.092	0.993
	0.83	0.002	0.398	0.055	0.980
Fe-1%C-3.75%Mn	0.43	0.004	0.426	0.005	0.998
	0.83	0.001	0.101	0.274	0.998

III.5 Deformation, Densification and Bulging

Fig. 14 has been drawn between the relative density (ρ_f/ρ_{th}) and the bulging ratio for all the steels compositions and both aspect ratios. Curves in this figure are found to be similar in characteristic features and, therefore, they can be represented by the similar mathematical expression. Curve fitting techniques attempted for the curves in this figure yielded a second order polynomial between relative density and the bulging ratio (D_b/D_0) of the form:

$$(\rho_f/\rho_{th}) = m_0 + m_1 (D_b/D_0) + m_2 (D_b/D_0)^2 \quad \text{..... .... (12)}$$

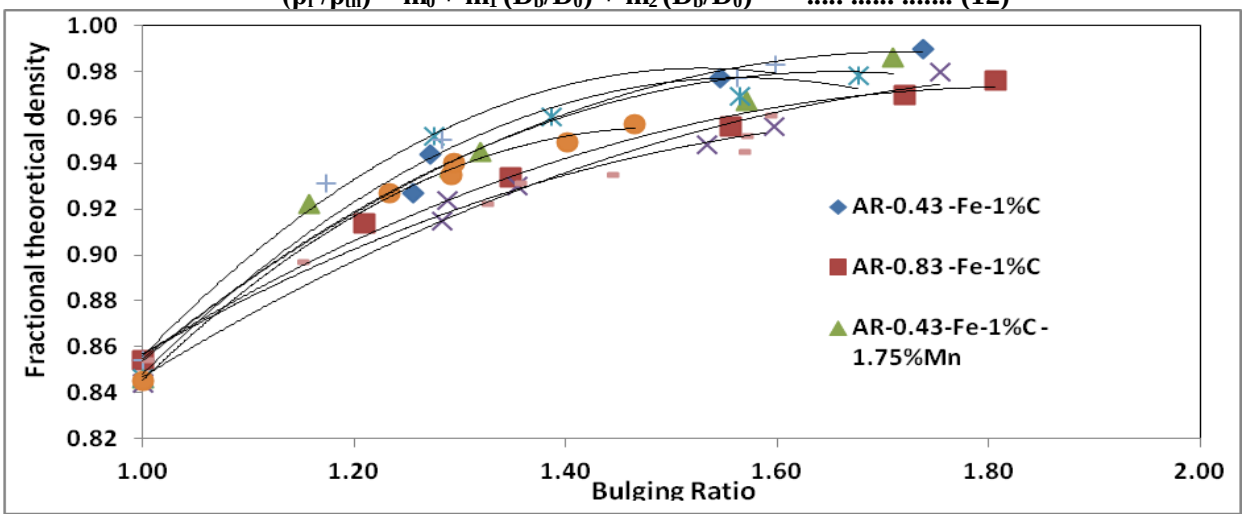

Figure 14 Effect of Initial Preform Geometry and Composition of Steels on the Relationship Between Fractional Theoretical Density and the Bulge Ratio (Db/D0) during Hot upset Forging of Sintered Fe-1% C-X Mn Steels.

Table 13 Coefficients of the Second Order Polynomial of the form: $\rho_f/\rho_{th} = m_0 + m_1 (D_b/D_0) + m_2 (D_b/D_0)^2$ Hot Upset Forging Sintered Fe - 1% C - X Mn P/M Steels of Different Initial Aspect Ratios

Composition	H/D	m_1	m_2	m_3	R^2
Fe-1%C	**0.43**	**-0.2531**	**0.8744**	**0.2332**	**0.9911**
	0.83	**-0.17**	**0.6215**	**0.4053**	**0.993**
Fe-1%C-1.75%Mn	**0.43**	**-0.292**	**0.968**	**0.1776**	**0.9607**
	0.83	**-0.1511**	**0.5852**	**0.4127**	**0.9826**
Fe-1%C-2.75%Mn	**0.43**	**-0.4014**	**1.258**	**-0.0085**	**0.983**
	0.83	**0.4595**	**1.369**	**-0.0641**	**0.9969**
Fe-1%C-3.75%Mn	**0.43**	**-0.4493**	**1.3734**	**0.0682**	**0.9918**
	0.83	**-0.1669**	**0.596**	**0.4277**	**0.9796**

III. 5.1 Power Law Relationship between [% (FTD)] and Bulging Ratio (D_b/D_0)

Fig. 15 is drawn between Log (%(ρ_f/ρ_{th})) and the Log (bulging ratio), i.e., Log (D_b/D_0) showing the influence of initial preform geometries during hot upset forging of sintered Fe-1.0%C-0.0%Mn, Fe-1.0%C-1.75%Mn, Fe-1.0%C, Fe-1.0%C-2.75%Mn and Fe-1.0%C, Fe-1.0%C-3.75%Mn sintered PM steel. It is

observed that all the data points exhibit straight lines in two distinct segments for a given aspect ratio and for the given steel. The corresponding slopes and the intercepts are reported in Table 13. In the first segment the values of the regression coefficients are exactly unity, therefore, the curve fitting carried out is perfectly ideal in this region. However, the regression coefficients in the second segments are beyond 0.9591 a minimum to 0.9951 a maximum value. Hence, it can be taken up as empirically as a very good curve fitting; the slopes of the lines in the respective segments are represented by p_1 and q_1.Whereas, the intercepts of the lines in the respective segments are denoted by p_2 and q_2 respectively. Thus, on conversion of these logarithmic lines into the power law equation format, a general power law equation that emerges out is given as beneath:

$$\{\% (\rho_f/\rho_{th})\} = P (D_b/D_0)^M \quad \text{..... (13)}$$

Where, $\{\% (\rho_f/\rho_{th})\}$ is per cent theoretical density achieved at a given height strain and (D_b/D_0) is the corresponding bulging ratio. P is the coefficient and M is the exponent of the power law equation. are already explained above. Thus, it is feasible to represent per cent theoretical density with the bulging ratio by a power law equation of the above form.

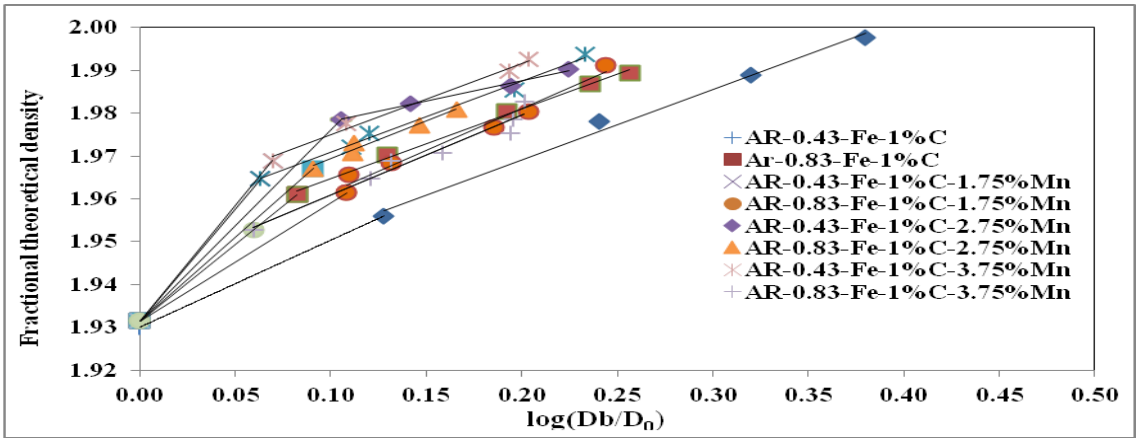

Figure 15 Influence of Initial Aspect Ratio and the Addition of Manganese in Fe - 1.0% C steel on the Relationship Between Log of {% (Relative Density)} and the Log of {Bulge Ratio (Db/D0)] in order to Establish if a Power Law Relationship Exists between Fractional Theoretical Density and the Bulge Radius.

Table 14 Coefficients Of the Lines and the intercepts Drawn Between Log(% Relative Density and the Log (Db/D0) in two Segments Exhibiting the Influence of Manganese Addition in Fe - 1.0%C Steel During Hot Upset Forging For Equation of the Form: Log (Relative Density) = (p_1 or q_1) Log (Db/D0) +Log (p_2 or q_2) i.e., the power Law Equation of the Form: % (ρf/ρth) = (p2 or q2) (Db/D0)$^{(p1 \text{ or } q1)}$

Composition	H/D	p_1	p_2	R^2	q_1	q_2	R^2
Fe-1%C	0.43	0.2034	1.93	1	0.165	1.9361	0.9927
	0.83	0.3572	1.9315	1	0.1627	1.9484	0.9951
Fe-1%C-1.75%Mn	0.43	0.5264	1.9315	1	0.1659	1.9543	0.9916
	0.83	0.2765	1.9315	1	0.1951	1.9421	0.9757
Fe-1%C-2.75%Mn	0.43	0.446	1.9315	1	0.0949	1.9686	0.99
	0.83	0.3916	1.9315	1	0.1765	1.9517	0.9693
Fe-1%C-3.75%Mn	0.43	0.5385	1.9315	1	0.1669	1.9583	0.9904
	0.83	0.1875	1.9422	1	0.1875	1.9422	0.9591

III.6 Deformation, Densification and Bulge Radius

Fig. 16 is drawn between the radius of curvature of bulging and the relative density (ρ_f/ρ_{th}) for all the four compositions and for all aspect ratios. Curve fitting technique has been attempted and it was established that all the curves conformed to a second order polynomial of the form:

$$R_c = n_0 + n_1 (\rho_f/\rho_{th}) + n_2 (\rho_f/\rho_{th})^2 \quad \text{... ... ... (14)}$$

Where, n_0, n_1 and n_2 are empirically determined constants and these constants are tabulated in Table 13. Above constants are further observed to depend upon the initial preform geometries and also upon the compositions of the systems selected in the present investigation. Further, the values of the regression coefficients (R^2) are found to be in very much close to unity, but, in few cases, the same is less than 0.95. Therefore, in these cases the curve fittings have been reasonably good whereas in other cases where R^2 values were beyond 0.999 and or above it, they had the best fit of the curves.

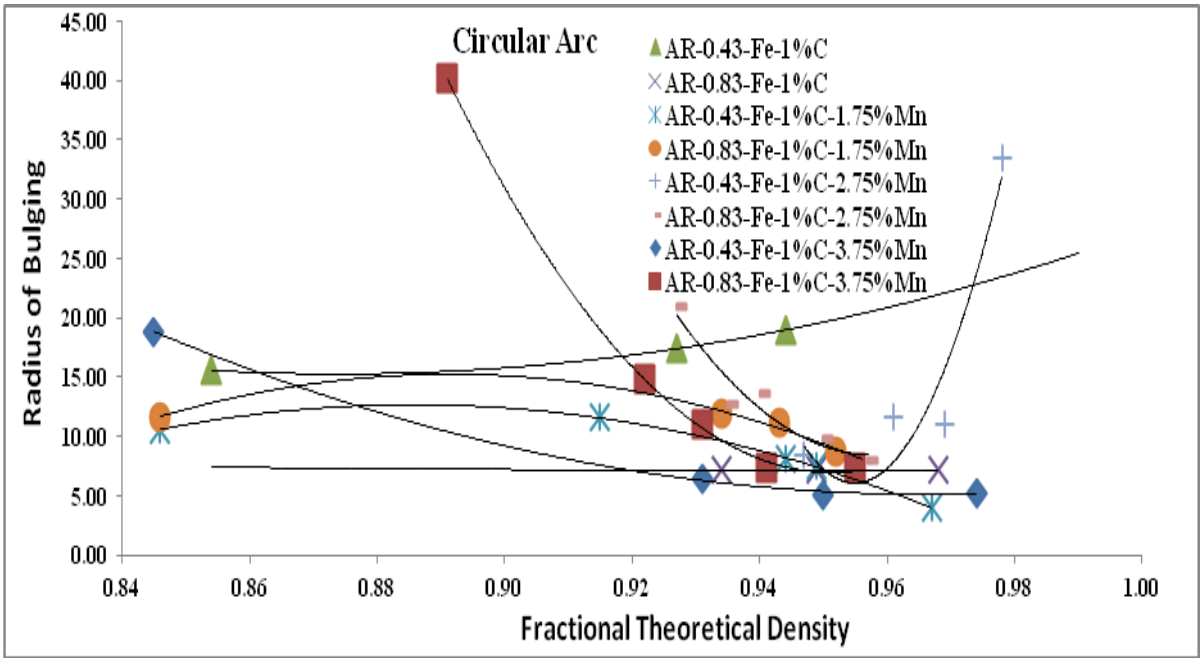

Figure 16 Effect of Initial Aspect Ratio (H_0/D_0) on the Relationship between Radius of Bulging and Fractional Theoretical Density for Circular Arc.

Table 15 Coefficient of the Polynomial of the form: $R_c = m_0 (\rho_f/\rho_{th}) + m_1 (\rho_f/\rho_{th}) + m_2 (\rho_f/\rho_{th})^2$

Composition	H/D	m_0	m_1	m_2	R^2
Fe-1%C	0.42	-1116	2314	-1179	1
	0.83	-560.1	1178	-612	0.999
Fe-1%C-1.75%Mn	0.42	-1018	2327	-1313	0.999
	0.83	-1347	3057	-1714	0.948
Fe-1%C-2.75%Mn	0.42	44349	-92868	48623	0.903
	0.83	11419	-23825	12436	0.922
Fe-1%C-3.75%Mn	0.42	875.3	-1801	931.8	0.999
	0.83	8284	-17403	9147	0.999

IV. CONCLUSIONS

Based upon the experimental data and the calculated parameters and series of plots drawn and their critical analysis have led to the following major findings:

A. Densification curves drawn between relative density and the true height strains were established to conform to a third order polynomial of the form:
$(\rho_f/\rho_{th}) = a_0 + a_1\epsilon_h + a_2\epsilon_h^2 + a_3\epsilon_h^3$; where, '$a_0$', '$a_1$', '$a_2$' and '$a_3$' were found to be empirically determined constants and dependent upon the initial preform geometries and the compositions of the steels. The constant 'a_0' did not contribute to densification as it corresponded to the initial preform relative density. 'a_1' linearly contributed to densification whereas the constants 'a_2' and 'a_3' moderated the densification in the final stages of deformation and densification. Since the values of regression coefficients (R^2) were found to be close to unity, hence, the above is the best empirical relation relating to the relative density and the true height strain.

B. Relative density (ρ_f/ρ_{th}) with respect to the normal diameter strain $\ln(D_{cf}/D_0)$ and the diameter strains considering circular and parabolic barrelling conformed to a second order polynomial of the form : $(\rho_f/\rho_{th}) = b_0 + b_1\epsilon_d + b_2\epsilon_d^2$ for normal deformation and $(\rho_f/\rho_{th}) = c_0 + c_1\epsilon_{dc} + c_2\epsilon_{dc}^2$ for circular barrelling, whereas, for parabolic arc of barrelling , a third order polynomial of the form : $(\rho_f/\rho_{th}) = d_o + d_1\epsilon_{dp} + d_2\epsilon_{dp}^2 + d_3\epsilon_{dp}^3$ existed. 'b_0', 'b_1', 'b_2', 'c_0', 'c_1', 'c_2', 'd_0', 'd_1', 'd_2' and 'd_3' were found to be empirically determined constants and dependent upon the initial preform geometries and the compositions of the steels investigated . 'b_0', 'c_0' and 'd_0' were found to be close to initial relative density (ρ_0/ρ_{th}) of the preform and, therefore, did not contribute to densification. 'b_1' and 'c_1' linearly assisted to densification whereas 'b_2' and 'c_2' being negative retarded the densification more effectively in the final stages of densification. Further, the constants 'd_1' and 'd_3' enhanced the densification on deformation whereas the constant 'd_2' being negative retarded the densification more effectively in the final stages of deformation and densification. Since the regression coefficient (R^2) values were found to be in very much close to unity, hence, the above empirical relations stand well established.

C. It is established that the Poisson's ratio for conventional, circular and parabolic barrelling during hot upset forging were found to be related to relative density (ρ_f/ρ_{th}) by a second order polynomial of general form as: $\upsilon_{pg/cir/para} = m_0 + m_1 (\rho_f/\rho_{th}) + m_2 (\rho_f/\rho_{th})^2$ where 'm_0', 'm_1' and'm_2' are empirically determined constants and are found to be functions of initial preform geometry and the steels compositions. Since the values of the regression coefficients (R^2) have been almost ideally unity, and, therefore, the empirically arrived relationship is highly justified. Further, it has been established that as the densification approached to cent per cent, the values of eth Poisson's ratio approached to an ideal value of 0.5 which means that during final stages of deformation and densification, the flow of pores and material became simultaneous.

D. Variation of true diameter strains whether it was for conventional or for circular or for parabolic barrelling, they all conformed to a second order polynomial with true height strains. The same were expressed by a general mathematical expression of the form: $\epsilon_{dg/cir/para} = s_0 + s_1\epsilon_h + s_2\epsilon_h^2$ where 's_0', 's_1'and 's_2' are empirically determined constants found to depend upon initial preform geometries and the steel compositions for respective mode of barrellings. The values of 's_0' was found to be zero or in close proximity to zero, hence, the above equation is simplified as: $\epsilon_{dg/cir/para} = s_1 + s_2\epsilon_h^2$. Further, the values of regression coefficient (R^2) where found to be almost unity, and hence, the above expression relating $\epsilon_{dg/cir/para}$ with the true height strain ($\epsilon_h = \ln(H_0/H_f)$ attains the highest degree of validity.

E. It was established that the relationship between relative density **(ρ_f/ρ_{th})** and the bulging ratio conformed to a second order polynomial of the form: $(\rho_f/\rho_{th}) = m_0 + m_1 (D_b/D_0) + m_2 (D_b/D_0)^2$, where '$m_0$', '$m_1$' and '$m_2$' are empirically determined constants and are found to be the functions of the initial preform geometries and the steel compositions taken for the present investigation. Further attempt also established that the % FTD can be expressed as a power law expression of the form: $(\%\ (\rho_f/\rho_{th})) = P (D_b/D_0)^M$, where, P and M are empirically determined constants and were found to depend upon the initial preform geometries and the steel compositions.

F. Arc radius of the barrel has been computed and the same was found to be related to the relative density(ρ_f/ρ_{th}) by a second order polynomial of the form: $R_b = n_0 + n_1(\rho_f/\rho_{th}) + n_2(\rho_f/\rho_{th})^2$ where 'n_0','n_1' and 'n_2' are empirically determined constants which depended upon the initial perform geometries and steels investigated. Regression coefficient values (R^2) were found to be in close proximity to unity and, hence, the above relationship stands well justified.

Thus, the present investigation comprehensively deals with the various aspects of hot deformation of hyper-eutectoid P/M steel showing the influence of manganese addition and initial aspect ratios of the preforms on the densification mechanism, different barrelling aspects, showing their typical influence on densification aspects and the variation between diameter strains (conventional, circular and parabolic arc of barrellings) and on the behaviour of Poisson's ratio. The present investigation has led to various new findings which are of paramount importance to the future investigators in the deformation of porous materials.

REFERNCES

[1]. Donald S. Clark and W. R. Varney, "Physical Metallurgy for Engineer", East- West Edition 1963, pp.226-247.

[2]. B. K. Agrawal, " Introduction to Engineering Materials", Tata McGrawHill Publishing Company Limited, New Delhi, 1989, pp.79-152.

[3]. G. S. Upadhaya, "Manganese in P/M Alloys", Ed. by the Manganese Centre, France, 1986, pp.9-52, 1986.

[4]. Donald G. White, "Exploring New P/M Horizons", International Journal of Powder Metallurgy, Vol.28, No.1, pp.229-232, 1992.
[5]. Peter K. Johnson, "P/M Applications Diversifying into New Markets", ibid, pp. 233-241.
[6]. Maurice A. Clegg, Joseph M. Capus, Roch H. Angers and John A. Lund, " Powder Metallurgy in Canada", ibid, pp. 149-258.
[7]. K. S. Pandey and R. Vijaya Raghavan, "Extrusion Forging of Indigenously Developed Iron - 0.25% Phosphorous Alloy Powder Preforms in Different Die Cavities," Quarterly International Journal of Powder Metallurgy Science and Technology, Vol.6, No.4, pp. 8-18, 1995.
[8]. K. S. Pandey, P. S. Mishra and M. L. Mehta, "Effect of Carbon Content on the Mechanical Properties of Material Science and Engineering , Vol.425, pp.367- 386, 2006.
[9]. R. Narayanasamy, V. Senthil Kumar and K. S. Pandey, "Some Aspects on Hot Forging of Powder Metallurgy Sintered High Strength 4% Titanium Carbide Composite Steel Preforms Under Different Stress State Conditions", Materials and Design, Vol.29,pp.1380-1400, 2008.
[10]. Bockstiegel G., Olsen H., "Processing Parameters in Hot Forging of Powder Preforms", 3rd European Powder Supplement Part-1, Powder Metallurgy 9, U.K., pp.127- 138, 1971.
[11]. H. F., Fischmeister, B. Aren and K. E. Easterling, "Deformation and Densification of Powder in Hot Forging ", Powder Metallurgy, Vol. 14, No.27, pp.144 - 163, 1971.
[12]. H. W. Antes, "Cold and Hot Forging P/M Preforms", SME, International Meeting, Philadelphia, Published as a Special SME Report, EMR71-01, pp.1 - 23, 1971.
[13]. Wang Junhua, Qi Jiazhong, Van Puyuan and Wange Enke, "Effect of Hot Repressing on the Mechanical Properties of Sintered Steels", Modern Developments in Powder Metallurgy, Edited by N. Aqua and Charles I. Whiteman, Vol.15, pp.639 - 653, 1984.
[14]. S. Mocarski, "Hardenable Hot Formed P/M Steels as a Substitute for Conventional Steels", International Journal of Powder Metallurgy, Vol.12, No.1, pp.47-57, 1976.
[15]. Darrell W. Smith, "Calculation of Pore Free Density of P/M Steels: Role of Microstructure and Composition ", International Journal of Powder Metallurgy, Vol.28, No.3, pp.259 - 269, 1992.
[16]. Eloff and E. Wilocox, " Modern Developments in Powder Metallurgy, Vol.7, Edited by H. H. Hausner and W. E. Smith, MPIF, Princeton, pp.213 - 233, 1974.
[17]. K. S. Pandey, "Die Design for Hot Forgings of Sintered Iron Powder Performs", Quarterly International Journal of Powder Metallurgy Science and Technology, Vol.4, No.1, pp.35-46, 1992.
[18]. K. S. Pandey, P. S. Mishra and M. L. Mehta, "Densification of Iron Powder Preforms During Hot Upsetting", Trans. of P.M.A.I., Vol.13, pp.94-99, 1986.
[19]. H. F. Fischmeister, et al “Deformation and Densification of Porous Preforms in Hot Forging”, Powder Metallurgy, Vol.14, No.27, 1971, pp.144-163.
[20]. H. A. Kuhn, “Deformation Processing of Sintered Powder Materials”, Powder Metallurgy Processing, Ed. By H. A. Kuhn and A. Lawley, Academic Press, New York, 1978, pp.99-138.
[21]. M. N. Rao and K. S. Pandey, “Working of Porous Solid Cylinders of Eutectoid Steel Composition”, 14th National AIMTDR Conference Proceedings, 1990, pp.217-222.
[22]. K. S. Pandey, “Feasibility of Hot Axial Forging of Sintered Hyper Eutectoid Steel”, 15th National
[23]. AMTDR Conference Proceedings, 1992, pp.D17/1-D17/6.
[24]. Upset Forged Iron Powder Preforms to square Cross -Section Bars", Quarterly International Journal of Powder Metallurgy Science and Technology, Vol.2, No.1, pp. 36-44, 1990.
[25]. K. S. Pandey, "Indigenously Developed and Modified Ceramic Coating", Department of Metallurgical and Materials Engineering, National Institute of Technology, Tiruchirappalli-620015, Tamil Nadu, India.
[26]. R. Narayanasamy, V. Senthil Kumar and K. S. Pandey, "Some Aspects of Workability Studies on Hot Forging of Sintered High Strength 4% Titanium Carbide Composite Steel Preforms", Journal of
[27]. . R. Narayanasamy and K. S. Pandey, “Some Studies on the Barrelling of Powder Preforms during Upsetting”, Quart. Int. J. of P/M Sci. and Tech., 1990, Vol.1, No.2, pp.10-23.
[28]. 27. R. Narayanasamy, M. Narayana Rao and K. S. Pandey, "Mathematical Treatment of Barrelling in Porous Solid Cylinders Under Axial Compression", Trans. of P.M.A.I., Vol. 20, 1993, pp. 33-4
[29]. The Above Article was reproduced In the Journal of Tools and Alloy Steels, Vol. 28, No.10, October 1994, pp. 292-297.
[30]. 28. R. Narayanasamy and K. S. Pandey, "Some Aspects of Barrelling of Porous Solid Cylinders of Iron
[31]. Powder Preforms during Axial Compression", Quarterly International Journal of Powder Metallurgy
[32]. Science and Technology, Vol. 1, No. 2, 1990, pp. 24-34.